

# An Examination of the Electron Densities in a Series of Tripodal Cobalt Complexes Bridged by Magnesium, Calcium, Strontium and Barium.

John Bacsa<sup>1,\*</sup>, Lillian G. Ramírez-Palma,<sup>2</sup> Fernando Cortés-Guzmán,<sup>2</sup> Christian M. Wallen,<sup>1</sup> and Christopher C. Scarborough<sup>1</sup>

<sup>1</sup> Department of Chemistry, Emory University, 1515 Dickey Dr., Atlanta, Georgia 30322, USA

<sup>2</sup> Instituto de Química, Universidad Nacional Autónoma de México, Circuito Exterior, Ciudad Universitaria, México, 04510, México; fercor@unam.mx

\* Correspondence: jrbacsa@emory.edu; Tel.: +1-404-727-6140

**Abstract:** X-ray crystallographic and theoretical charge density data for a series of compounds  $[(\text{Co}(\text{Ts}_3\text{tren}))\text{M}(\text{Co}(\text{Ts}_3\text{tren}))]$  ( $\text{M} = \text{Mg}, \text{Ca}, \text{Sr}$  and  $\text{Ba}$ ) is examined. The crystal structures are isostructural and the alkaline earth metal ions have the same arrangement of donor oxygen atoms despite the large variation in ionic radii. The isomorphism of these molecules is surprising and a theoretical examination of the electronic structures, with the different metal ions along the series, provides detailed insight into their stabilities. The theoretical and experimental data are consistent and agree well. The local properties of the  $\text{Co}(\text{II})$  ion and its donor atoms are relatively independent of the alkali earth metal.

**Keywords:** QTAIM; alkaline earth metals; theoretical electron densities.

## 1. Introduction

Spectroscopic and electrochemical data and preliminary X-ray crystallographic data for the series of compounds  $[(\text{Co}(\text{Ts}_3\text{tren}))\text{M}(\text{Co}(\text{Ts}_3\text{tren}))]$  ( $\text{M} = \text{Mg}, \text{Ca}, \text{Sr}$  and  $\text{Ba}$ ) were reported (1). The results show that the cobalt(II) anions are in an unusual four-coordinate environment which is trigonally pyramidal. The fourth nitrogen atom above the triangle of three nitrogen atoms forms the apex of the trigonal pyramid but the fifth site in the potential trigonal bipyramid is vacant and instead a redox-inert alkaline earth metal is nearby. The alkaline earth metal bridges two trigonal pyramidal cobalt(II) anions. The bridging symmetry is enforced by a crystallographic inversion center. Six oxygen atoms, three from three Ts groups of one  $[(\text{Co}(\text{Ts}_3\text{tren}))]^{1-}$  complex and another three from the second  $[(\text{Co}(\text{Ts}_3\text{tren}))]^{1-}$  bind to the alkaline earth metal. The triangles of three oxygen atoms above and below the alkaline earth metal are twisted through an angle of  $45^\circ$  relative to one another about the vertical axis (the Co-M-Co axis), forming an trigonal antiprism and an overall octahedral arrangement of oxygen atoms. The crystal structures are isostructural and the  $\text{M}^{2+}$  ions have the same arrangement of six sulfonamido oxygen atoms. The isomorphism of these molecules is surprising because the magnesium and barium atoms are so different. Barium atoms favor much higher coordination numbers with weaker interactions. Because a six-coordinate  $\text{Mg}^{2+}$  ion is much more stable than a six-coordinate  $\text{Ba}^{2+}$  ion it is reasonable to assume there is distortion and stress in the Ba-crystal. Thus appreciable differences in the energies are expected across this series of compounds. The crystals of the Mg-compound were of the best quality but most of the crystals of the Sr and Ba-compounds were twinned and the structures were disordered. The disordered crystals are made up of intimate components that are rotated about each other along the  $c$ -axis. We hypothesize that stress in the compounds with the larger ions may distort the crystal lattices causing crystallographic defects. Interestingly, although the neighboring domains possess different orientations, the splitting of the domains within the crystal coincides exactly with the  $c$ -axis giving a hexagonal packing motif. The disorder is borne out by twinning by inversion. The differences in the stabilities of the isomorphous compounds are also borne out by the reactivity studies which show the

Ba-compound to be the least stable and the most vulnerable to hydrolysis (1-3). The poor solubility of the Mg complex precluded its inclusion in the hydrolysis experiments but the observed trend is  $\text{Ba} < \text{Sr} < \text{Ca}$ , so it is reasonable to expect that the Mg complex is also the most stable to hydrolysis. We were interested to see whether the electronic nature of the cobalt ions and whether the donor-character of the sulfonamido oxygen donors changes when the small acidic  $\text{Mg}^{2+}$  ion is replaced by bigger ions especially because the identity of the alkaline earth metal plays a prominent role in catalysis (2-9) but spectroscopic profiling of the interactions between these redox-inert metals with the cobalt-supporting ligand through electron-rich sulfonamido oxygen donors is challenging. Elucidating the origin of the redox-inert metal-ion effect is critical to the potential development of these compounds as catalysts for industrially important transformations. Spectroscopic and electrochemical techniques have been employed to examine the cobalt chromophore, but these studies have not revealed any differences in the electronic structure of the cobalt ion as a function of the identity of the alkaline earth metal. Therefore, charge density studies of these compounds using diffraction data from single crystals and from quantum mechanical calculations were performed. These electron densities were analyzed using the quantum theory of atoms in molecules (QTAIM)(10). Specifically, local properties at the bond critical points and atomic charges, for the cobalt ions, sulfonamido oxygen donors, and alkaline earth metals were compared and trends examined. Delocalisation indices were calculated to examine the basic pattern of interactions between the alkali earth metals and the donor oxygen atoms and with the interactions between Co atoms separated by the alkali earth metal. The amount of electron sharing between atom basins *i.e.* the degree of delocalisation was derived from the exchange density. The delocalization indices between two atomic basins gave reasonable indications between the formal bond orders between the atoms in the complexes. These results show the effects of the  $\text{M} = \text{Mg}, \text{Ca}, \text{Sr}$  and  $\text{Ba}$  substitution on the electron density distribution and hence their potential catalytic activity. We find that, although the alkali metals have a dramatic effect on the reactivity and stabilities of these compounds, they have a very small observable effect on the transition metals. The energy differences of the isolated molecules were found to be small with similar electron distributions about the cobalt atoms (except for the Ba compound which has a stronger axial Co-N bond).

## 2. Materials and Methods

Theoretical electron density of  $[\text{C}_{36}\text{H}_{78}\text{MCo}_2\text{N}_8\text{O}_{12}\text{S}_6]$ , where M is Mg, Ca, Sr or Ba, was obtained at the M06-2X/DZP-DKH theoretical level. The M06-2X functional performs reasonably well when benchmarked against both CCSD(T) and experimental results for structures, dissociation energies and vibrational frequencies of alkaline-earth compounds (11). The DZP-DKH (Douglas-Kroll-Hess) is a contracted Gaussian basis sets of double zeta valence qualities plus polarization functions, with the contraction coefficients optimized using the relativistic DKH Hamiltonian for elements from H to Kr (12) and from Cs to Rn (13). This theoretical level allows us to analyze and compare the complexes with the four alkaline-earth metals. The set of Kohn-Sham molecular orbitals of each complex was obtained with Gaussian 09 software (14), and the local and integrated properties of electron density were calculated with the AIMAll suite of programs (15). Charge-density quality X-ray data was accessible for the Mg and Ca complexes but not the other compounds due to issues related to crystal quality and twinning. Multipolar refinements (16) were applied with a multipole expansion of the valence shell up to hexadecapoles for the Co, S, Mg, Ca, O and N atoms. Hartree-Fock functions were used for the core and spherical valence densities. Conventional refinements where the charge-density parameters  $P_v$ ,  $P_{lm}$ ,  $\kappa$  were optimized on the experimentally measured X-ray structure factors were carried out (17). The charge-density parameters  $P_v$ ,  $P_{lm}$ ,  $\kappa$  were also obtained for the Co, S, O and N atoms from non-relativistic wave function calculations by a published procedure (18). In this procedure density functional calculations are performed on the experimental charge density optimised atomic coordinates. The program TONTO (19) was used to calculate the structure factors from the theoretical electron density. The differences in the orbital populations derived from the experimental data and theoretical densities are within 1%.

### 3. Results

#### 3.1. The Crystal Structures of $[(Co(Ts3tren))M(Co(Ts3tren))]$

Although the dimeric cobalt(II) complexes bridged by alkali earth metals are isostructural, the smaller metals are more ordered, with the Mg and Ca compounds being the most ordered and well crystallized of the series. The molecular structure of the Mg compound, shown in Figure 1, will be discussed in the most detail. The molecule is located on a 3-fold rotation axis through the atoms Mg(1), Co(1) and N(1). Each magnesium ion is served as a bridge between two Co atoms and forms a very interesting column along the *c*-axis. As these atoms are situated on the rotation axis, the entire N(1)-Co(1)---Mg---Co(1)'-N(1)' system is linear within experimental error by crystallographic symmetry. Both Co---Mg distances are equal to 3.408(1) Å. Each Co atom is coordinated to four N atoms in a trigonal pyramidal arrangement with  $C_{3v}$  symmetry. The implication is that the symmetry of orbitals on the two cobalt atoms (and the apical N atoms) will be constrained by the crystallographic symmetry and will also have local symmetry  $C_{3v}$ . However, we did not impose this 3-fold symmetry in the quantum mechanical calculations but we did retain the overall inversion symmetry of the molecule during the calculations. In the multipolar model, the spherical harmonics functions with  $m = 1, 2, 4$  will be forbidden but  $m = 0, 3$  are allowed for this symmetry. An interesting feature, from a bonding and charge density perspective, is that the cobalt atom is missing an apical ligand *i.e* there is no ligand forming a bipyramid for dative bonds to cobalt. The electron-rich sulfonamido oxygens are a long distance from the Co atom (2.966(3) Å in the Ca compound and 2.863(3) Å in the Mg compound). Instead there is a  $M^{2+}$  ion at the apical position. Interactions between the Co and these sulfonamido oxygen cannot be ruled out and one of the aims of this charge density study was to determine the nature and extent of these interactions. The M-O bonds are expected to be completely ionic and it is unlikely to be any spin coupling between the Co(II) cations. The spin state was investigated using optimisations of unrestricted wavefunctions and the distributions of the spin densities in the molecule were visualized. The spin state was found to be (nearly) exactly  $S=3/2$  at each cobalt atom corresponding to a high-spin  $d^7$ -configuration. The unrestricted value of *S* was 3.0023 for the entire complex and NMR spectroscopy confirmed the assignment of  $S=3/2$  (1).

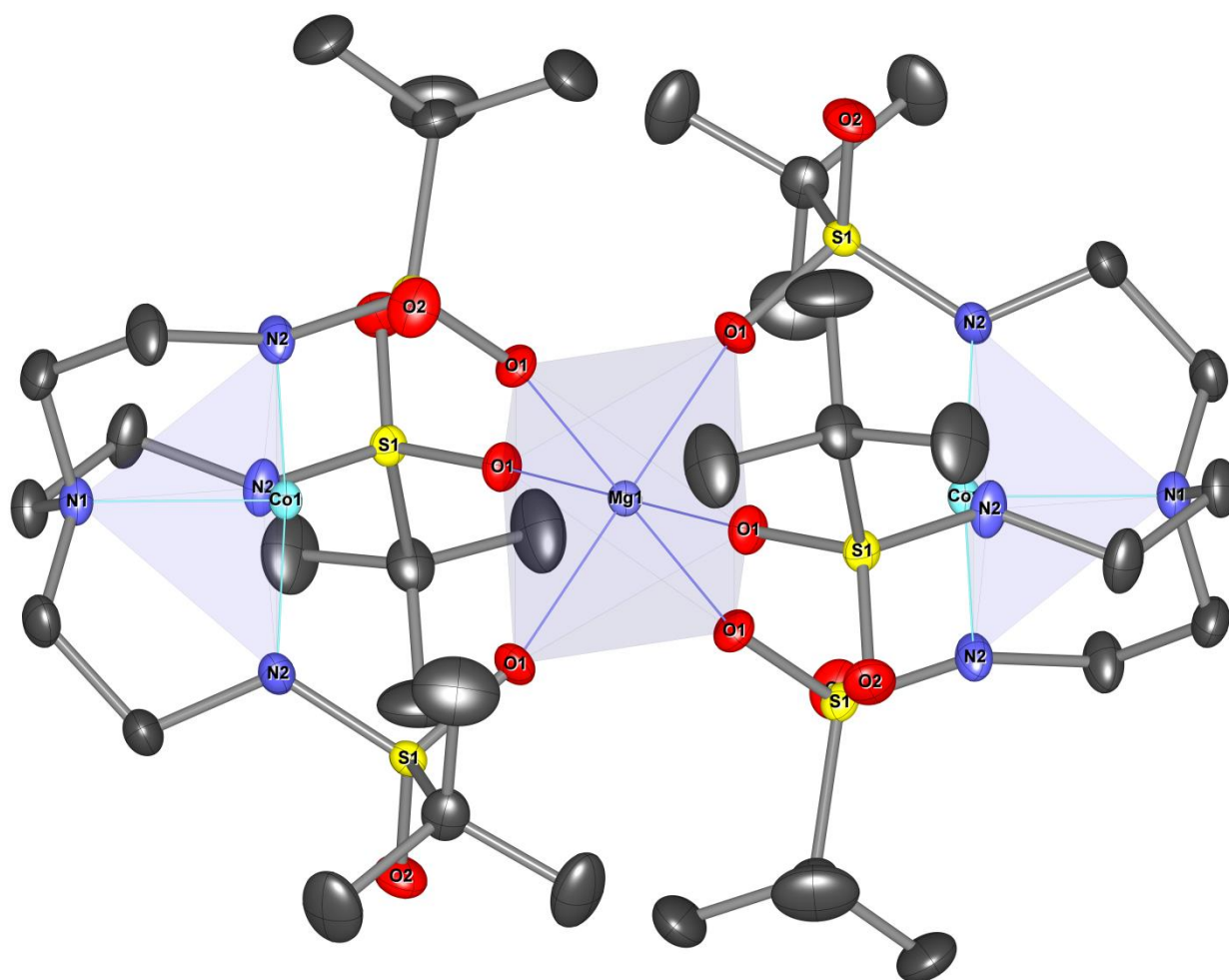


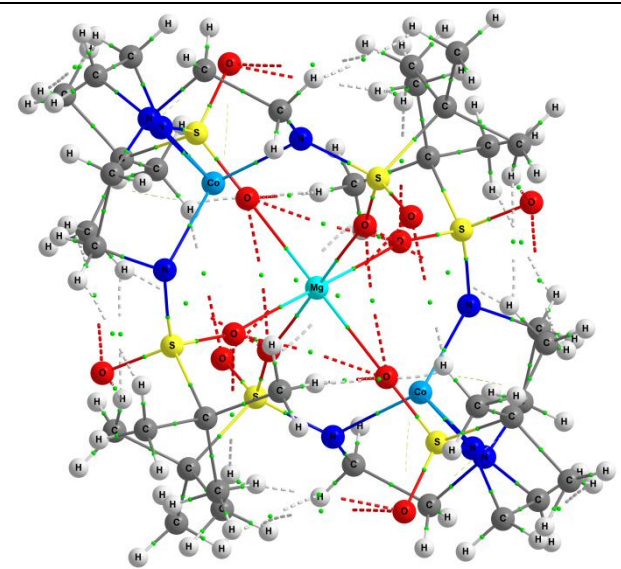
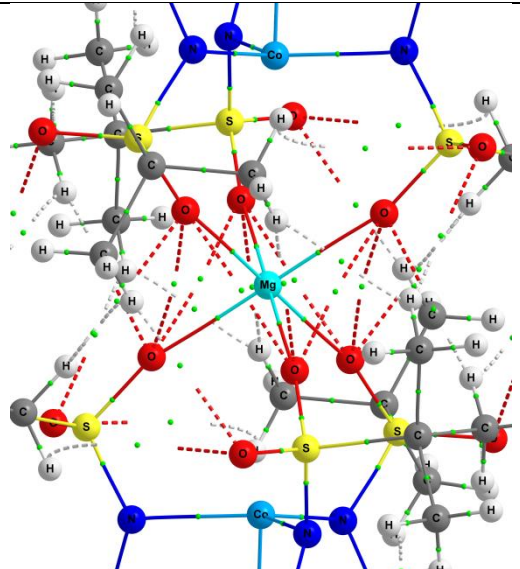
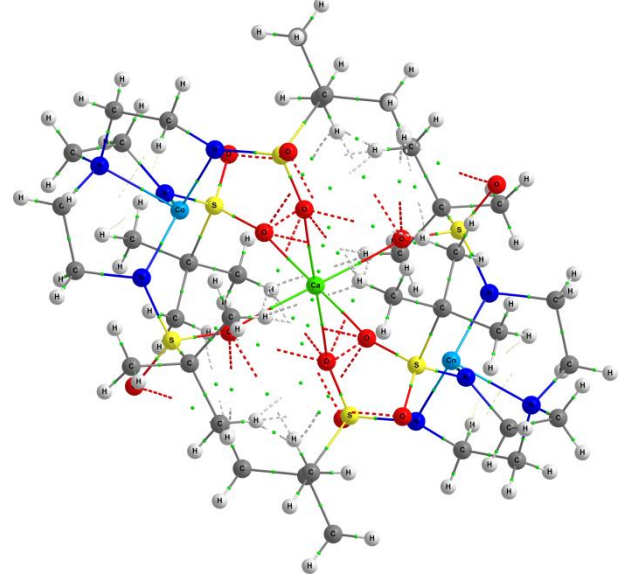
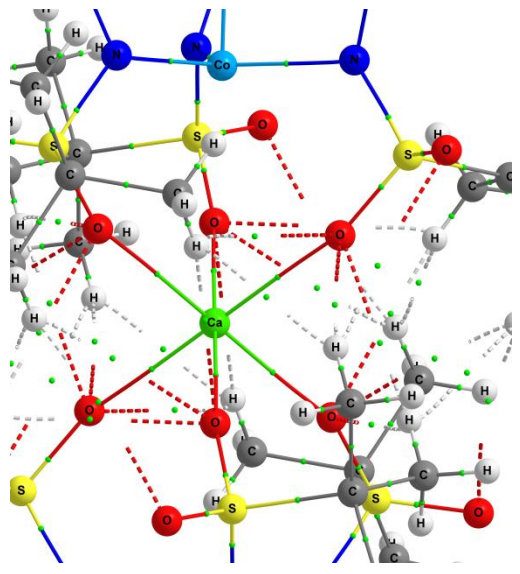
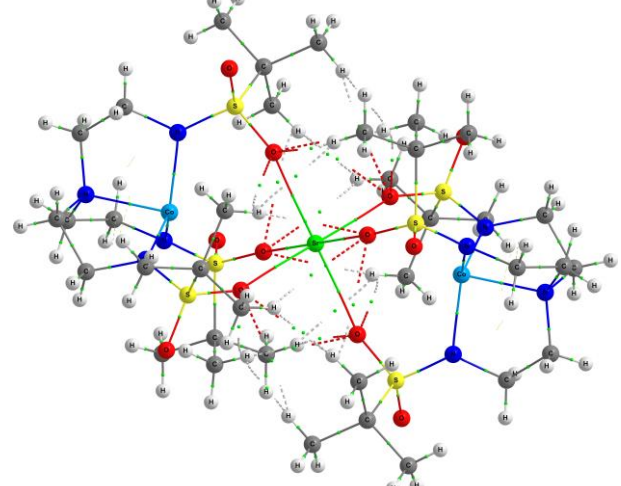
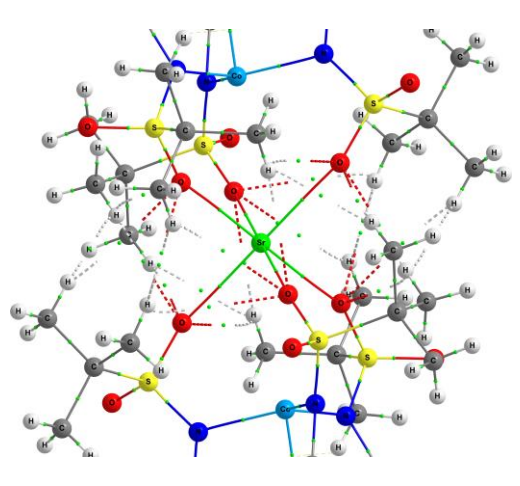
**Figure 1:** Thermal Ellipsoid Plot of the dimeric  $\text{Co}^{2+}$  complex  $[(\text{Co}(\text{Ts}_3\text{tren}))\text{Mg}(\text{Co}(\text{Ts}_3\text{tren}))]$ . Thermal ellipsoids are shown at the 79% probability level.

### 3.2. Theoretical Charge Density Analysis of $[\text{C}_{36}\text{H}_{78}\text{MC}_2\text{N}_8\text{O}_{12}\text{S}_6]$

Table 1 shows the molecular graphs (10, 20) of  $[\text{C}_{36}\text{H}_{78}\text{MC}_2\text{N}_8\text{O}_{12}\text{S}_6]$  for each alkaline-earth metals, where it is possible to observe, beside the covalent structure, an octahedral coordination sphere with six gradient paths between the alkaline-earth metal and the sulfonamido oxygens. The small coordination sphere of Mg allows the presence of a path between adjacent oxygen atoms, which also are involved in non-conventional hydrogen bonds (21).



Table 1. Molecular graph of the complexes.

Metal	Full molecular graph	Partial molecular graph (zoom)
Mg		
Ca		
Sr		

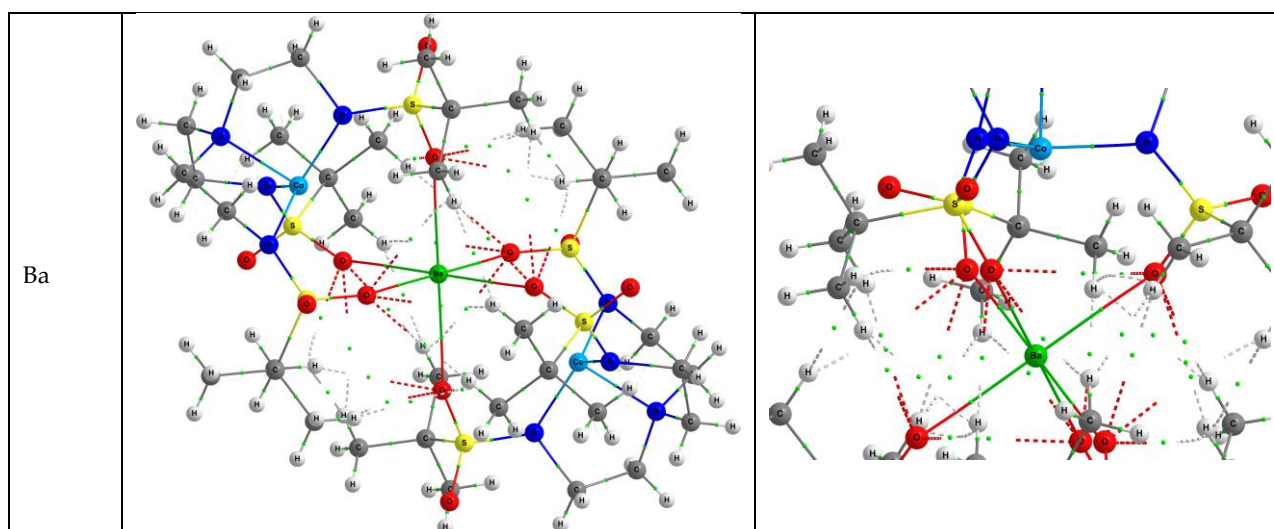
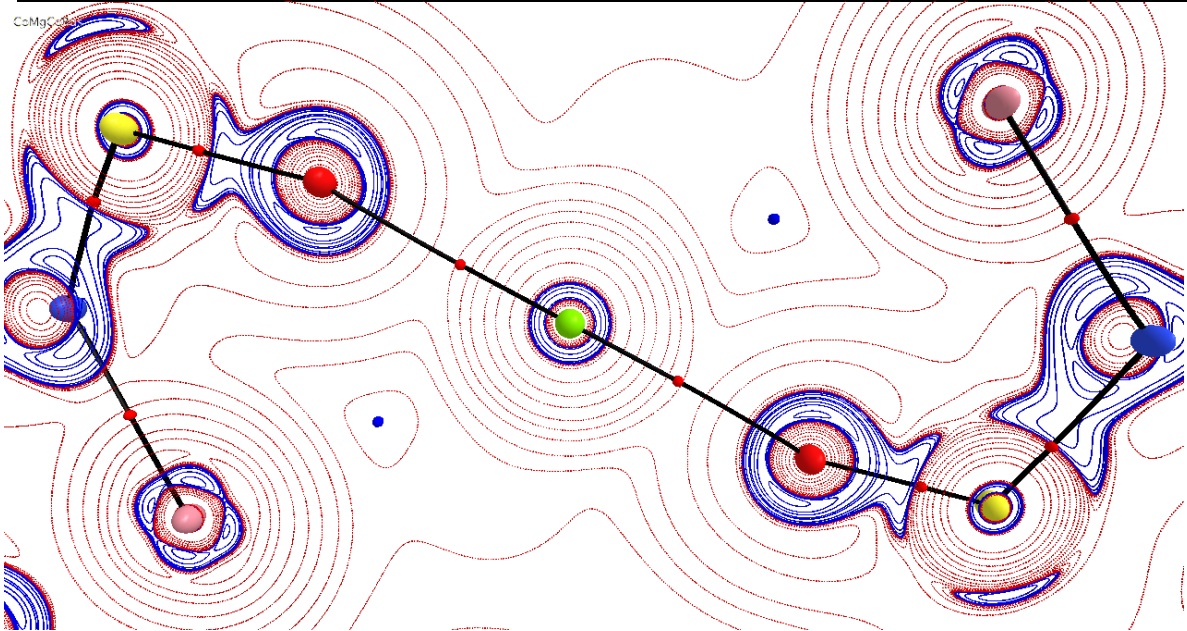


Table 2 presents the local properties at the bond critical points of selected interactions included in the molecular graph. In general, the alkaline-earth metal-oxygen interactions can be classified as closed shell interactions with low values of electron and electronic energy densities, along with positive values of Laplacian of electron density(22). These local properties agree with an ionic character of the alkaline-earth metal-oxygen interactions and the configuration of the coordination sphere around the metal follows Gillespie's rules (23). There are some trends in the local properties, the charge depletion ( $\nabla^2\rho_{\text{bcp}}$ ) decreases with the atomic number (Z) of the alkaline-earth metal, reducing the ionic character of the interaction ( $(\nabla^2\rho_{\text{bcp}} = -0.0015 Z + 0.2462, R^2 = 0.93)$ ). One can obtain the same conclusion from the energy density, where potential energy density increases with the atomic number. The electron delocalization between alkaline-earth metal and the oxygen atom increases as the covalent contribution does. The O-O contacts observed in the  $\text{MgL}_2$  complex present features of very weak, closed-shell interactions. On the other hand, the coordination sphere of the cobalt center is composed of four bond paths with nitrogen atoms of the ligand in a trigonal pyramid configuration. On the basis of the properties of the bond critical points, Co-N interactions present the features of directional metal ligand interactions (24). In general, equatorial ligands are strongly bonded to the cobalt atom (larger values of electron density and its Laplacian), except in the complex with barium, which presents a stronger axial metal-ligand interaction.

**Table 2.** Properties of the bond critical points and delocalization of M-O and Co-N interactions.

M <sup>2+</sup>	ρ <sub>bcp</sub>	∇ <sup>2</sup> ρ <sub>bcp</sub>	ε	H <sub>bcp</sub>	DI(M O)
	M··O				
Mg	0.0282	0.2330	0.0016	0.0103	0.0793
Ca	0.0326	0.2170	0.0158	0.0065	0.1293
Sr	0.0330	0.1799	0.0259	0.0045	0.1676
Ba	0.0305	0.1707	0.0279	0.0047	0.1630
	Co-N				
Mg	0.0976 0.0697	0.4739 0.3618	0.2631 0.0005	-0.0233 -0.0108	0.5127 0.3350

Ca	0.0991	0.4851	0.2683	-0.0237	0.5232
	0.0710	0.3725	0.0005	-0.0112	0.3375
Sr	0.0924	0.4469	0.2688	-0.0203	0.5074
	0.0725	0.3775	0.0009	-0.0118	0.3463
Ba	0.0889	0.4419	0.1913	-0.0189	0.4634
	0.0972	0.4740	0.2859	-0.0225	0.5228



**Figure 2:** A contour map of the of the Laplacian of electron density in the plane of the Mg, Co and donor oxygen atoms in the dimeric Co<sup>2+</sup> complex [(Co(Ts<sub>3</sub>tren))Mg(Co(Ts<sub>3</sub>tren))]. The two small blue spheres are (3,+3) critical points, local minima of the electron density between the magnesium and cobalt atoms.

The contour map of the Laplacian of electron density of MgL<sub>2</sub>, displayed in figure 2, shows the spherical distribution of the charge concentration within the valence shell of the magnesium atom. Also it is possible to observe the polarization of the valence shell of the cobalt metal center, with the charge depletions directed toward the charge concentrations of the nitrogen atoms. An interesting feature of the molecular graphs is the interatomic region between the magnesium and cobalt atoms, where an axial charge depletion of the cobalt valence shell faces a (3,+3) critical point, a local minimum of the electron density. This feature is also observed in the other complexes.

**Table 3.** Molecular graph of the complexes

Metal	Full molecular graph	Partial molecular graph (zoom)
-------	----------------------	--------------------------------



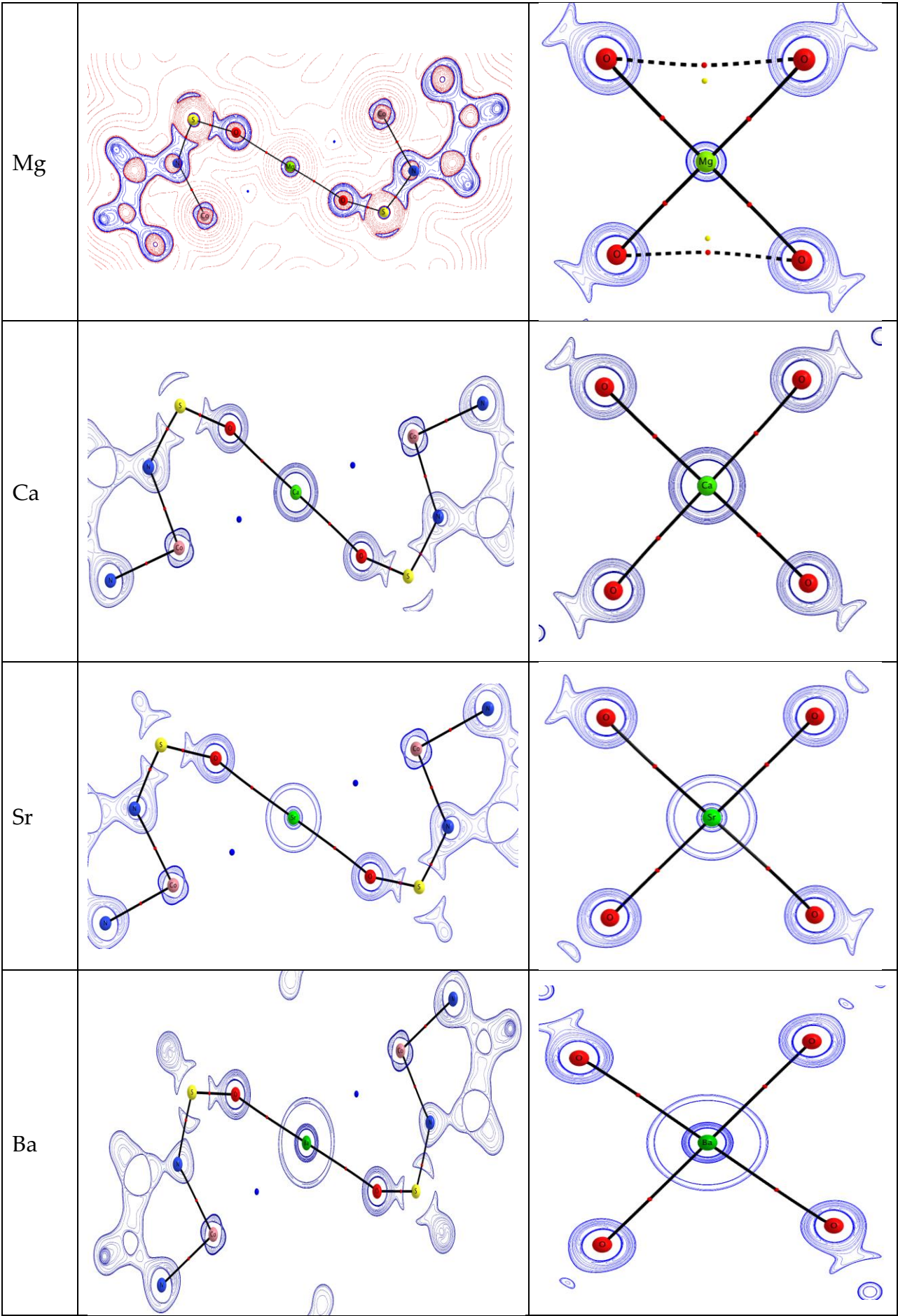




Table 4 presents selected atomic properties useful to show the influence of the alkaline-earth metal to the cobalt metal center. There is a nonlinear correlation between the atomic number of the alkaline-earth metals and its electron delocalization (DI) within the molecule ( $y = -0.0003 DI^2 + 0.0256 DI + 0.0044$ ,  $R^2 = 0.99$ ). The delocalization with the linked atoms by bond paths ( $DI_B$ ) presents the same correlation. Also, it is possible to observe correlations between non bonded delocalization ( $DI_{NB}$ ) and the atomic number ( $DI_{NB} = 1 \times 10^{-05} Z^2 - 0.0015 Z + 0.2082$ ,  $R^2 = 0.99$ ). There is a correlation between  $DI_B$  of the alkaline-earth metal ( $DI_B(M)$ ) and the  $DI_{NB}$  of the cobalt atom ( $DI_{NB}(Co)$ ), where an increment of  $DI_B(M)$  is associated with an decrease of  $DI_{NB}(Co)$ .

**Table 4.** Integrated properties of  $M^{2+}$  and Co atoms

Atom		q(A)	N(A)	LI(A)	DI	$DI_B$	$DI_{NB}$	E(A)
$M^{2+}$	Mg	1.8168	10.1832	9.924	0.2591	0.2378	0.0213	-199.2018
	Ca	1.8158	18.1842	17.7603	0.4239	0.4058	0.0181	-676.1906
	Sr	1.7665	36.2335	35.6785	0.5550	0.5027	0.0523	-3108.0289
	Ba	1.9283	54.0717	53.5193	0.5523	0.4892	0.0631	-8363.3441
Co	Mg	1.3174	25.6826	24.5528	1.1297	0.9365	0.1933	-1379.8770
	Ca	1.3133	25.6867	24.5496	1.1372	0.9535	0.1836	-1380.2187
	Sr	1.3118	25.6882	24.5805	1.1077	0.9342	0.1735	-1381.6302
	Ba	1.3098	25.6902	24.5639	1.1263	0.9565	0.1699	-1242.0423

### 3.2. Visualisation and Qualitative Analysis of the Deformation Density of the $[(Co(Ts3tren))M(Co(Ts3tren))]$ complexes

Visually, the qualitative character of the deformation ED appears to be very similar for the Mg, Ca, Sr and Ba compounds. A deformation electron density map in the plane of the  $Ca^{2+}$  atom and two of the donor oxygen atoms and in the plane of the  $Co^{2+}$  atom and two of the donor nitrogen atoms (Figure 3). Four charge concentrations corresponding to the d-electrons about the cobalt atoms are visible. These are asymmetric and appear to be more dominant on the side facing the  $Mg^{2+}$  ion. A representation of the three-dimensional deformation density showing the character of the chemical bonding for the Ca compound is shown in Figure 4. There are concentrations of charge corresponding to the d and lone pair electrons. The deformation density about  $M^{2+}$  is very nearly spherical showing the purely ionic character of this atom. The contour map in a cross section through the Ca and two O atoms shows the minimal perturbation of the ED by the donor oxygen atoms. However, there is a complex distribution of charge about the  $Co^{2+}$  atom. There is an annular region of charge depletion in the xy-plane containing the three equatorial N atoms. In simple crystal field theory, d-electrons in this region are repulsed by the electrostatic field of the N atoms and the d-energy levels are expected to be higher and their populations lower in this region of the crystal field. In contrast, there are two nearly equivalent annular regions with local charge concentrations at angles subtended by the equatorial xy-plane and the axial z-axis (containing the axial N atom). In each of these two regions there are three maxima of charge. Two nearly equivalent regions of charge depletion are present in the axial direction directed both toward the axial N atom and toward the Ca atom. The charge depletions appear to be smaller than the equatorial depletions. The two axial charged depletions are almost the same although one is directed towards an axial ligand. This distribution of charge is what is expected on the basis of a simplified classical crystal field picture of bonding. In trigonal bipyramidal ( $C_{3v}$ ) geometry, we would expect the  $dx^2-y^2$  and  $dxy$  orbitals to be the most destabilized, while the  $dxz$  and  $dyz$  to be degenerate and the lowest in energy, and the  $dz^2$  in the middle. This arrangement does depend on the relative donor strength of the sulfonamido and amine donors.

### 3.2. Comparison of some experimentally and theoretically derived parameters

Theoretical and experimental multipolar parameters for cobalt are compared in Table 5. D-orbital populations were obtained from the multipole populations and are given in Table 6.

**Table 5.** The monopole populations, radial parameters, multipolar coefficients (dipoles, quadrupoles, octupoles and hexadecapoles) and atomic charges for cobalt (from X-ray data (1) and theoretical densities (2)). Some coefficients are zero because of site symmetry 3.

	1	2
Pval	7.675(58)	7.077
Kappa	0.996(6)	1.003
Net charge	-0.435	-0.037
D10	-0.218(22)	0.004
Q20	0.227(30)	0.176
Q30	-0.102(19)	0.001
Q40	-0.371(30)	-0.387
O32-	0.05(2)	-0.001
H40	0.27(3)	0.235
H43+	-0.087(27)	-0.045
H43-	0.068(27)	-0.108

**Table 6.** The d-orbital populations (%) obtained from X-ray data (1) and from the theoretical multipolar parameters theoretical densities (2).

Orbital	1	2 (Mg)	2 (Ca)
$z^2$	16.2	15.0	16.6
xz	26.2	26.4	25.4
yz	26.2	26.4	24.2
$x^2-y^2$	15.7	16.1	17.0
xy	15.7	16.2	16.8

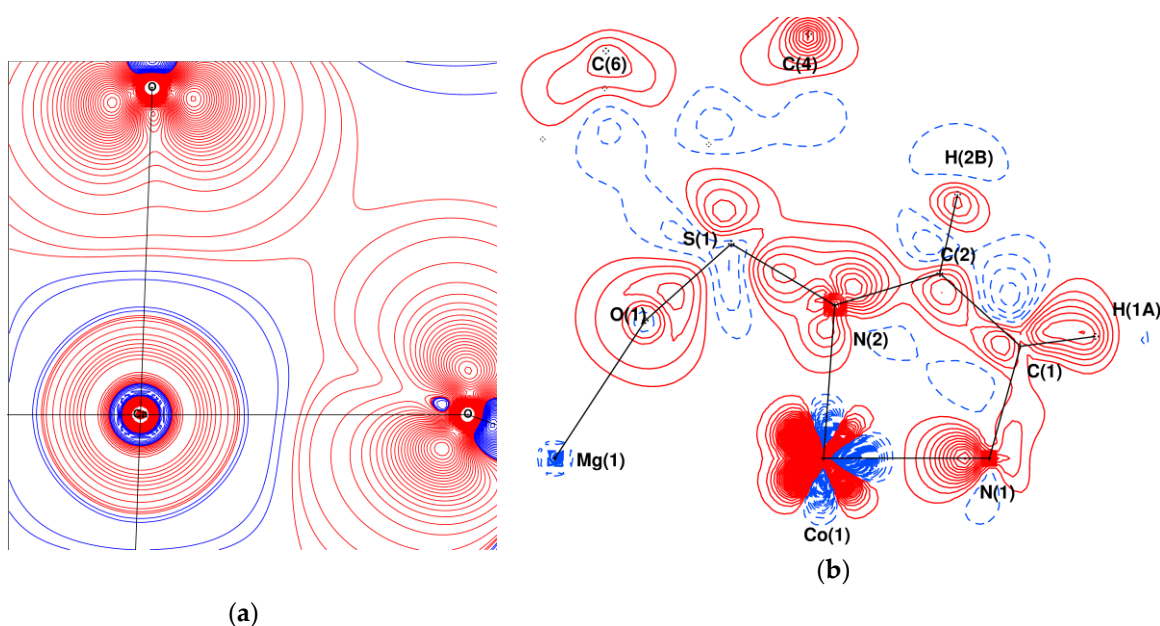


**Figure 3.** (a) A deformation electron density map in the plane of the  $\text{Ca}^{2+}$  atom and two of the donor oxygen atoms. The density is almost perfectly spherical about the calcium and two lobes of density corresponding to the two pairs of lone pair electrons about each oxygen are visible. Red lines represent positive contours and blue lines represent negative contours. Contours are drawn at  $0.1 \text{ e}\text{\AA}^{-3}$  intervals. (b) A deformation electron density map in the plane of the  $\text{Co}^{2+}$  atom and two of the donor nitrogen atoms. Four charge concentrations corresponding to the d-electrons about the cobalt atoms are visible and two of these are larger towards the  $\text{Mg}^{2+}$  ion. Red lines represent positive contours and blue lines represent negative contours. Contours are drawn at  $0.1 \text{ e}\text{\AA}^{-3}$  intervals.

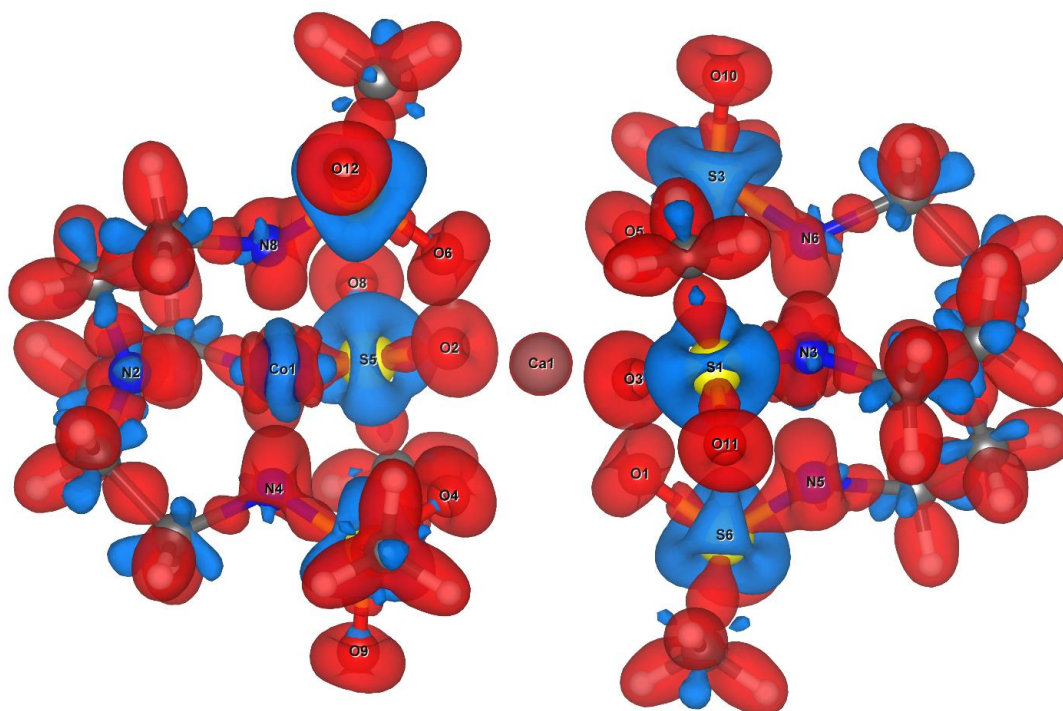


**Figure 4.** (a) Positive and negative deformation density isosurfaces ( $0.02 \text{ e}\text{\AA}^{-3}$ ) of the dimeric  $\text{Co}^{2+}$  complex  $[\text{C}_{36}\text{H}_{78}\text{CaCo}_2\text{N}_8\text{O}_{12}\text{S}_6]$  from refinements with the predicted multipolar parameters. Charge concentrations are shown in red and depletions in blue.

## 5. Conclusions

Accurate mapping of the electron density provided an experimental probe of the interactions around alkaline earth metal. The delocalization indices between two atomic basins gave reasonable indications between the formal bond orders between the atoms in the complexes. The differences in the common atomic properties across the series are small (despite large differences in the stabilities of these compounds). The net atomic charges (Table 4) of the  $\text{M}^{2+}$  ions are in the range +1.78 to +1.93 and there is no clear trend in the variation of charges. Atomic charges for the cobalt(II) atoms are nearly identical across the series (+1.31). It is worth noting that there is an uneven increase in bond delocalization indices across the series (Mg (0.2378), Ca (0.4058), Sr (0.5027) and Ba (0.4892)) with a sudden increase between magnesium and calcium. These indices give a measure of the amount of sharing of electrons between the magnesium and the donor oxygen atoms. The atomic charges of the donor oxygen atom to the  $\text{M}^{2+}$  ions are very similar (-1.46). We find that, although the alkali metals have a dramatic effect on the reactivity and stabilities of these compounds, they a very small

observable effect on the transition metals. The energy differences of the isolated molecules were found to be small with similar electron distributions about the cobalt atoms (except for the Ba compound which has a stronger axial Co-N bond). The differences in reactivity need to be understood by examining the amount of energy released on forming the reaction products (appreciably less energy might be released in forming the hexa-aqua  $\text{Mg}^{2+}$  ion than the fully hydrated  $\text{Ba}^{2+}$  ion from the  $[(\text{Co}(\text{Ts}_3\text{tren}))\text{M}(\text{Co}(\text{Ts}_3\text{tren}))]$  compounds). However, there are subtle differences in the electron density distributions in the Co-O-Mg-O-Co planes and in the bond critical points around the Co atom, and in the molecular graph of the Mg-compound. The slight variations indicate that a complete study of the reactivities of these compounds should include an analysis of the reaction products and that QTAIM does not necessarily predict *a priori* the relative stabilities of molecules.

**Acknowledgments:** We thank acknowledge the Emory X-ray Crystallography Facility for the X-ray structural analysis. We also acknowledge the use of the Rigaku SYNERGY-S diffractometer with a HYPIX detector, supported by the National Science Foundation under grant CHE-1626172. We also acknowledge DGTIC-UNAM for the computer time (grant LANCAD-UNAM-DGTIC-194). John Bacsá acknowledges the use of the resources of the Cherry L. Emerson Center for Scientific Computation.

**Author Contributions:** Christopher Scarborough and Christian Wallen prepared the compounds and performed the reactivity studies; John Bacsá carried out the diffraction experiments and analysed the data; Lillian G. Ramírez-Palma and Fernando Cortés-Guzmán carried out the theoretical studies; John Bacsá, Fernando Cortés-Guzmán and Christian Wallen wrote the paper

**Conflicts of Interest:** The authors declare no conflict of interest.



## References

1. Wallen CM, Wielizcko M, Bacsá J, Scarborough CC. Heterotrimetallic sandwich complexes supported by sulfonamido ligands. *Inorganic Chemistry Frontiers*. 2016;3(1):142-9.
2. Wallen CM, Bacsá J, Scarborough CC. Coordination of Hydrogen Peroxide with Late-Transition-Metal Sulfonamido Complexes. *Inorganic Chemistry*. 2017.
3. Bang S, Lee Y-M, Hong S, Cho K-B, Nishida Y, Seo MS, et al. Redox-inactive metal ions modulate the reactivity and oxygen release of mononuclear non-haem iron(III)-peroxo complexes. *Nat Chem*. 2014;6(10):934-40.
4. Hong S, Pfaff FF, Kwon E, Wang Y, Seo M-S, Bill E, et al. Spectroscopic Capture and Reactivity of a Low-Spin Cobalt(IV)-Oxo Complex Stabilized by Binding Redox-Inactive Metal Ions. *Angewandte Chemie International Edition*. 2014;53(39):10403-7.
5. Lee Y-M, Bang S, Kim YM, Cho J, Hong S, Nomura T, et al. A mononuclear nonheme iron(III)-peroxo complex binding redox-inactive metal ions. *Chemical Science*. 2013;4(10):3917-23.
6. Miller CG, Gordon-Wylie SW, Horwitz CP, Strazisar SA, Peraino DK, Clark GR, et al. A Method for Driving O-Atom Transfer: Secondary Ion Binding to a Tetraamide Macrocyclic Ligand. *Journal of the American Chemical Society*. 1998;120(44):11540-1.
7. Monte-Pérez I, Kundu S, Ray K. An Open-Shell Spin Singlet Copper-Nitrene Intermediate Binding Redox-innocent Metal Ions: Influence of the Lewis Acidity of the Metal Ions on Spectroscopic and Reactivity Properties. *Zeitschrift für anorganische und allgemeine Chemie*. 2015;641(1):78-82.
8. Park YJ, Cook SA, Sickerman NS, Sano Y, Ziller JW, Borovik AS. Heterobimetallic complexes with MIII-([small mu ]-OH)-MII cores (MIII = Fe, Mn, Ga; MII = Ca, Sr, and Ba): structural, kinetic, and redox properties. *Chemical Science*. 2013;4(2):717-26.
9. Yao S, Xiong Y, Vogt M, Grützmacher H, Herwig C, Limberg C, et al. O<sub>2</sub> Bond Activation in Heterobimetallic Peroxides: Synthesis of the Peroxide [LNi( $\mu_2$ - $\eta^2$ -O<sub>2</sub>)K] and its Conversion into a Bis( $\mu$ -Hydroxo) Nickel Zinc Complex. *Angewandte Chemie International Edition*. 2009;48(43):8107-10.
10. Bader RFW. *Atoms in Molecules: A Quantum Theory*; Clarendon Press; 1990.
11. Sun Z, Launder AM, Schaefer HF. Prediction and Characterization of Alkaline-Earth (M=Be, Mg, Ca, Sr, and Ba) Metallacyclopentadienes and Relevant Derivatives. *ChemistrySelect*. 2017;2(4):1442-53.
12. Jorge FE, Neto AC, Camiletti GG, Machado SF. Contracted Gaussian basis sets for Douglas-Kroll-Hess calculations: Estimating scalar relativistic effects of some atomic and molecular properties. *The Journal of Chemical Physics*. 2009;130(6):064108.
13. Martins LSC, Jorge FE, Franco ML, Ferreira IB. All-electron Gaussian basis sets of double zeta quality for the actinides. *The Journal of Chemical Physics*. 2016;145(24):244113.
14. Frisch MJ, Trucks GW, Schlegel HB, Scuseria GE, Robb MA, Cheeseman JR, et al. *Gaussian 16 Rev. B.01*. Wallingford, CT2016.
15. Keith TA. AIMAll 17.11.14 ed. TK Gristmill Software, Overland Park KS, USA, 20172017.
16. Hansen NK, Coppens P. Testing aspherical atom refinements on small-molecule data sets. *Acta Crystallographica Section A*. 1978;34(6):909-21.
17. Koritsanszky T HS, Su Z, Mallinson P. R., Richter T. & Hansen, N. K. XD2006 - a Computer Program Package for multipole Refinement and Analysis of Electron Densities from Diffraction Data. 2006.
18. Bacsá J, Briones J. Determination of the electron density in methyl ( $\pm$ )-(1S, 2S, 3R)-2-methyl-1, 3-diphenylcyclopropanecarboxylate using refinements with X-ray scattering factors from wavefunction calculations of the whole molecule. *Acta Crystallographica Section C: Crystal Structure Communications*. 2013;69(8):910-4.
19. Jayatilaka D, Grimwood DJ, editors. *Tonto: A Fortran Based Object-Oriented System for Quantum Chemistry and Crystallography*2003; Berlin, Heidelberg: Springer Berlin Heidelberg.
20. Bader RFW. A quantum theory of molecular structure and its applications. *Chemical Reviews*. 1991;91(5):893-928.
21. Alkorta I, Rozas I, Elguero J. Non-conventional hydrogen bonds. *Chemical Society Reviews*. 1998;27(2):163-70.

22. Macchi P, Sironi A. Chemical bonding in transition metal carbonyl clusters: complementary analysis of theoretical and experimental electron densities. *Coordination Chemistry Reviews*. 2003;238-239:383-412.
23. Gillespie RJ, Robinson EA. Models of molecular geometry. *Chemical Society Reviews*. 2005;34(5):396-407.
24. Cortés-Guzmán F, Bader RFW. Complementarity of QTAIM and MO theory in the study of bonding in donor–acceptor complexes. *Coordination Chemistry Reviews*. 2005;249(5):633-62.